Shape Modeling of Continuous-Curvature Continuum Robots

Shaoping Bai

Abstract An essential problem in developing concentric-tube continuum robots is to determine the shape of the robot, which is dependent on robot structure and external load. A comprehensive model that takes into considerations of influencing factors is hence required. In this work, the shape modeling of a type of concentric-tube continuum robot built with a collection of super-elastic NiTiNol tubes is studied. The model, developed on the basis of differential geometry and curved beam theory, is able to determine both the bending deflection and torsional deformation for a continuum robot of continuous curvature. Simulation results for calculating the shape of a continuum robot built with NiTiNol tubes are included.

Key words: Kinematics of flexible manipulators, continuous-curvature continuum robots, shape modeling, NiTiNol tubes

1 Introduction

Continuum robots encompass new principles of robot inspired by the nature. A continuum robot is a robot that is able to deform continuously, similar to their counterparts in nature such as snakes, elephant trunks or octopus arms. The continuum robots are able to move in any direction, both laterally and axially, or even 'turning corner'. Contrary to traditional robots built with rigid links, a continuum robot is constructed with a collection of flexible structures which allow them deform locally to generate desired motion.

The continuum robots can be built with different principles, as seen in some prototypes including multi-sectional pneumatic actuating robot Air-Octor[1], fluid-driven Octpus Arm[2], tendon-driven robots[3], among others. Of these robots, robots with concentric tubes of NiTiNol (Nickel-Titanium) alloy are more promising for applications where a super mobility in a confined space is critical, such as the robotic minimally invasive surgery, due to the relative simple structure, compact size (diameters can be as small as a few millimeters), and bio compatibility to human tissues. A number of modeling works on continuum robots were reported[4, 5, 6]. The models were mainly developed on the basis of Cosserat rod with either en-

Shaoping Bai
Department of Mechanical and Manufacturing Engineering & Centre for Robotics Research, Aalborg University, Denmark
e-mail: shb@m-tech.aau.dk

ergy approach or variational methods [7, 8]. An approach of including torsion was proposed by Dupont et al. in [9]. In most works, shape models were derived by assuming piecewise-constant curvatures.

In this work, the problem of shape modeling for continuum robots built with concentric tubes is addressed, focusing on the geometrically exact model of the robot shape. In this modeling work, both the bending deflection and torsional deformation are considered. As the shape model is derived on the basis of continuous curvatures, a more comprehensive and accurate model for the continuum robot can be obtained, compared with the piecewise constant curvature approach. Simulations were carried out to demonstrate the application of the model.

The paper is organized as follows. Section 2 describes the geometry of a spatial curve and a single tube, upon which the equilibrium condition of a two-tube assembly is established. The shape modeling of continuum robots is presented in Section 3. Simulation results are reported in Section 4. The work is concluded in Section 5.

2 Model of a single spatial tube

A continuum robot can be built with multiple sessions of concentric tubes, as demonstrated in Fig. 1, which can be considered as a combination of several sections serially connected. In each session, two tubes of different diameters are assembled with variable configuration and thus build the desired shape. The shape modeling of continuum robots can thus be built on the shape calculation of a single tube.

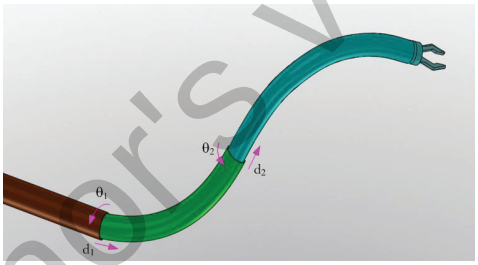

Fig. 1 A continuum robot built with multiple sessions of concentric tubes

2.1 Geometry of a spatial curve

A space curve $\mathscr{C}$ can be expressed as a function of arc length s, i.e., $\mathscr{C} : \mathbf{r} = \mathbf{r}(s), s \in \mathbb{R}$. At any point s, the derivative of the function $\mathbf{r}(s)$ with respect to s is equal to the tangential vector of the curve, i.e. $\mathbf{t} = d\mathbf{r}/ds$, as shown in Fig. 2. Together with

the normal vector $\mathbf{n}$ at s, and a third vector $\mathbf{b} = \mathbf{t} \times \mathbf{n}$, the *Frenet-Serret* frame, or *F-S* frame in short, is fully established. The shape function of a space curve can be described by the Frenet-Serret equation[10] in matrix form

$$\mathbf{T}' = \mathbf{T}\widetilde{\boldsymbol{\kappa}}; \quad \widetilde{\boldsymbol{\kappa}} = \begin{bmatrix} 0 & -\tau & \kappa \\ \tau & 0 & 0 \\ -\kappa & 0 & 0 \end{bmatrix} \tag{1}$$

where $\mathbf{T} = [\mathbf{n}, \mathbf{b}, \mathbf{t}]$ and $\boldsymbol{\kappa} = [0, \kappa, \tau]^T$ is a vector of curvatures. Here, and in the balance of the paper, the prime symbol denotes the derivative with respect to arc length s, and $\widetilde{\boldsymbol{\kappa}}$ is the cross-product matrix (a skew-symmetric matrix) of the vector $\boldsymbol{\kappa}$.

The F-S frame admits kinematic meanings. In fact, if the F-S frame slides along the curve at a unit velocity, the value of $\boldsymbol{\kappa}$ is the angular rate of the frame about $\mathbf{b}$, while τ is the angular velocity about $\mathbf{t}$. The vector $\boldsymbol{\kappa} = [0, \kappa, \tau]^T$, if interpreted in terms of velocity, is the local velocity expressed in the F-S frame. The global counterpart of $\boldsymbol{\kappa}$ can be found by $\boldsymbol{\kappa}_{global} = \mathbf{T}\boldsymbol{\kappa}$.

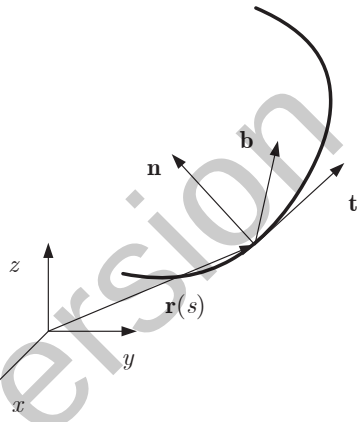

Fig. 2 A spatial curve and its associated Frenet-Serret frame

The F-S frame is unique, which satisfies the Frenet-Serret equation and describes entirely the curve shape. For a continuum tube, however, the material twist at a cross-section has to be described in order to determine the tube's torsional deformation. In light of this, a frame along the center line has to describe the twist of the tube, in addition to the shape of the curve. In another words, a frame attached to the tube but different from the F-S frame is required. In this case, the vector of curvatures will be transformed due the change of the reference (view) frame, as shown in the following.

Let the F-S frame be noted as $\mathscr{T}$ corresponding to an orientation matrix $\mathbf{T}$. Assume there is another reference frame $\mathscr{F}$ of orientation matrix $\mathbf{F}$. The transformation from $\mathscr{T}$ to $\mathscr{F}$ is described by $\mathbf{F} = \mathbf{RT}$, where $\mathbf{R}$ is a rotation matrix. Let the vector of curvatures be $\boldsymbol{\lambda}$ when the curve is viewed from the reference frame $\mathscr{F}$. The following relationship between $\boldsymbol{\lambda}$ and $\boldsymbol{\kappa}$ can be found

$$\mathbf{R}^T\boldsymbol{\kappa} + \boldsymbol{\omega} = \boldsymbol{\lambda} \tag{2}$$

where $\boldsymbol{\omega}$ is the relative velocity of $\mathscr{F}$ frame with respect to the $\mathscr{T}$ frame. The alternative reference frame in this case is called an adapted frame.

A simple case is the adapted frame is obtained by rotating the F-S frame about $\mathbf{t}$ for an angle of α. Letting the new frame is noted by three orthogonal unit vectors $\{\mathbf{x}, \mathbf{y}, \mathbf{z}\}$ and $\mathbf{z}$ is parallel to $\mathbf{t}$, eq.(2) becomes

$$\mathbf{R}_z(\alpha)^T \boldsymbol{\kappa} + \alpha' \mathbf{e}_z = \lambda \tag{3}$$

where $\mathbf{R}_z(\alpha)$ is the matrix of rotation about z-axis. It can be known from eq. (3) that a curve of curvature of κ and torsional rate τ, when viewed in an adapted frame, has a vector of curvature $\boldsymbol{\kappa} = [\kappa \sin\alpha, \kappa\cos\alpha, \tau + \alpha']^T$.

2.2 Equilibrium equations

When a tube is subject to forces, an equilibrium condition is established after deformation. Refer to Fig. 3 where a small piece of a spatial rod is shown, the equation of moment equilibrium is derived as

$$d\mathbf{m} + \mathbf{e}_z ds \times \mathbf{f} = 0 \tag{4}$$

where $\mathbf{e}_z = [0,0,1]^T$. Noting that $\mathbf{m}$ in this equation is expressed in a moving adapted frame, care has to be given to both the variation of the vector and the frame as well. That means

$$d\mathbf{m} = \mathbf{m}' ds + \boldsymbol{\kappa} \times \mathbf{m} ds \tag{5}$$

Finally, we have

$$\mathbf{m}' + \boldsymbol{\kappa} \times \mathbf{m} + \mathbf{e}_z \times \mathbf{f} = \mathbf{0} \tag{6}$$

The second term in the left-hand side of equation (6) accounts for the effect of the tube's torsion. Likewise, the force equilibrium equation is found as

$$\mathbf{f}' + \boldsymbol{\kappa} \times \mathbf{f} = \mathbf{0} \tag{7}$$

Assume the rod deflection is subject to the linear elasticity theory and the axial

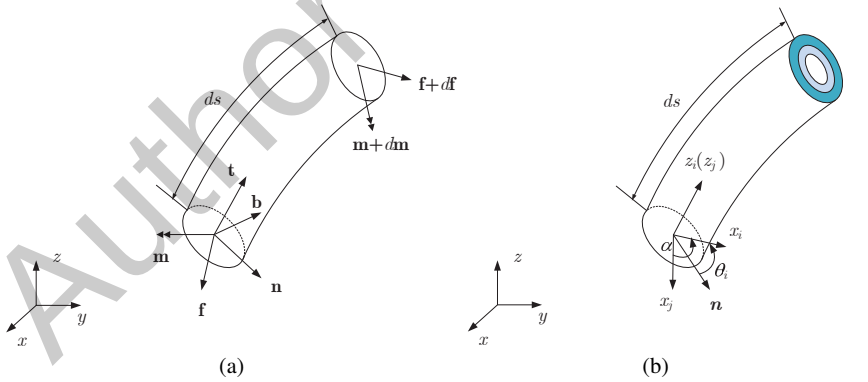

Fig. 3 Equilibrium condition, (a) a small piece of single spatial curved rod, (b) an assembly of two concentric tubes

extension can be ignored, we could concern about only the moment equilibrium equation. In this regard, the constitutive equation for the space rod subject to bending and torsional moments is

$$\mathbf{m}(s) = \mathbf{K}(\kappa(s) - \bar{\kappa}), \quad \text{with } \mathbf{K} = \begin{bmatrix} k_x & 0 & 0 \\ 0 & k_y & 0 \\ 0 & 0 & k_z \end{bmatrix} = \begin{bmatrix} EI & 0 & 0 \\ 0 & EI & 0 \\ 0 & 0 & GJ \end{bmatrix} \tag{8}$$

where $\bar{\kappa} = [\bar{\kappa}_x, \bar{\kappa}_y, \bar{\tau}]^T$ is the vector of initial curvature of the tube. E and G are the material's elastic (Young) and shear modulus, while I and J are the area and polar moment of inertia at a cross section, respectively.

3 Shape modeling of assembled tubes

When two tubes are assembled, they build a constrained mechanical system. To describe the deformation of each tube, local frames are established on each tube, which are able to describe the shape of their centerline and also the tube twist. The two local(adapted) frames are only different in twist angle, as demonstrated in Fig.3b.

For each segment of the tube assembly, the internal moments are balanced, i.e.,

$$\mathbf{m}_1(s) + \mathbf{R}_z(\alpha)\mathbf{m}_2(s) = 0 \tag{9}$$

with

$$\mathbf{m}_i = \mathbf{K}_i(\kappa_i - \bar{\kappa}_i), \quad i = 1,2 \tag{10}$$

In this case, $\kappa_i = [\kappa_{ix}, \kappa_{iy}, \tau_i]^T$, $\bar{\kappa}_i = [\bar{\kappa}_{ix}, \bar{\kappa}_{iy}, \bar{\tau}_i]^T$ for $i = 1,2$. Moreover, the mechanical constraint implies that two tubes' center lines superpose on each other, with only difference in torsional twist. In other words, eq. (3) has to be satisfied:

$$\mathbf{R}_z(\alpha)^T \kappa_1(s) + \alpha' \mathbf{e}_z = \kappa_2(s) \tag{11}$$

where α is the relative twist angle, as demonstrated in Fig.3b, which is defined as

$$\alpha(s) = \theta_2(s) - \theta_1(s) \tag{12}$$

where $\theta_i, i = 1,2$ is the twist angle of the i-th adapted frame measured with respect to the F-S frame. Both equations (9) and (11) are derived in a local frame. We rewrite eq.(11) as

$$\kappa_1(s) = \mathbf{R}_z(\alpha)(\kappa_2(s) - \alpha' \mathbf{e}_z) \tag{13}$$

Substituting equations (10) and (13) into (9) yields

$$\mathbf{K}_1(\mathbf{R}_z(\alpha)\kappa_2 - \alpha' \mathbf{R}_z(\alpha)\mathbf{e}_z - \bar{\kappa}_1) + \mathbf{R}_z(\alpha)\mathbf{K}_2(\kappa_2 - \bar{\kappa}_2) = 0 \tag{14}$$

Noting that a special identity $\mathbf{K}_1\mathbf{R}_z(\alpha) = \mathbf{R}_z(\alpha)\mathbf{K}_1$ exists for the tubes, due to the fact that the diagonal stiffness matrix $\mathbf{K}_1$ contains identical bending stiffness for x– and y– directions, we finally obtain

$$\kappa_2 = (\mathbf{K}_1 + \mathbf{K}_2)^{-1}(\mathbf{R}_z^T(\alpha)\mathbf{K}_1\bar{\kappa}_1 + \mathbf{K}_2\bar{\kappa}_2 + \alpha'\mathbf{K}_1\mathbf{e}_z) \tag{15}$$

Obviously, the shape of the tube assembly is fully determined if α and α' can be solved. To this end, we first expand eq. (15), which yields

$$\kappa_{2x} = \frac{E_1I_1\bar{\kappa}_{1y}\sin\alpha + E_1I_1\bar{\kappa}_{1x}\cos\alpha + E_2I_2\bar{\kappa}_{2x}}{E_1I_1 + E_2I_2} \tag{16}$$

$$\kappa_{2y} = \frac{-E_1I_1\bar{\kappa}_{1x}\sin\alpha + E_1I_1\bar{\kappa}_{1y}\cos\alpha + E_2I_2\bar{\kappa}_{2y}}{E_1I_1 + E_2I_2} \tag{17}$$

Recall that the third equation of eq.(6) is about the twist of tubes, which can be rewritten as

$$G_iJ_i\theta_i'' + \kappa_{ix}E_iI_i(\kappa_{iy} - \bar{\kappa}_{iy}) - \kappa_{iy}E_iI_i(\kappa_{ix} - \bar{\kappa}_{ix}) = 0, \quad i = 1,2 \tag{18}$$

that is

$$\theta_i'' = \frac{E_iI_i}{G_iJ_i}(\kappa_{ix}\bar{\kappa}_{iy} - \kappa_{iy}\bar{\kappa}_{ix}) \tag{19}$$

Substituting eqs. (16) and (17) into (19) and finally into equation

$$\alpha''(s) = \theta_2''(s) - \theta_1''(s) \tag{20}$$

yields

$$\alpha''(s) = A\cos\alpha(s) + B\sin\alpha(s) \tag{21}$$

where

$$A = \frac{E_1I_1E_2I_2(G_1J_1 + G_2J_2)}{G_1J_1G_2J_2\,(E_1I_1 + E_2I_2)}(\bar{\kappa}_{1x}\bar{\kappa}_{2y} - \bar{\kappa}_{1y}\bar{\kappa}_{2x}) \tag{22}$$

$$B = \frac{E_1I_1E_2I_2(G_1J_1 + G_2J_2)}{G_1J_1G_2J_2\,(E_1I_1 + E_2I_2)}(\bar{\kappa}_{1x}\bar{\kappa}_{2x} + \bar{\kappa}_{1y}\bar{\kappa}_{2y}) \tag{23}$$

Differential equation (21) can be solved with boundary conditions (BCs). For fixed-free ends, the BCs are

$$\alpha(0) = \theta_2(0) - \theta_1(0), \alpha'(l) = 0 \tag{24}$$

When a load is applied at the free end, the boundary conditions will change. The loaded cases require further detailed formulation and will be discussed in a separate paper.

The differential equation (21) is now ready to be solved with a numerical solver. With the curvature and the changing rate of twist angle found, the tube-assembly's shape can be uniquely determined for any given initial configuration at the end $s = 0$.

Equation (21) is the governing equation of the torsion for the tube assembly. The equation is different from the results reported in [9] (eq. (24)), as seen in the different coefficients. This is due to the fact that the new model is not limited to assemblies of tubes of constant curvatures as the approach in [9]. Instead, the new model can be applied to tube assembly of continuous curvatures, thus has a more general use in the shape calculation of continuum robots.

4 Simulations

The continuum robot in this work is built with concentric tubes of NiTiNol (Nickel-Titanium) alloys (NiTi SE 508). The outer tube has a diameter of 1.6mm and thickness of 0.2mm, while the inner tube is 1.32mm in diameter and 0.225mm in thickness, as listed in Table 1. The area and polar moments of inertia of the tubes can be calculated with the tube geometric parameters.

Table 1 Physical and geometric parameters of tubes

	Parameter	Value	Description
Physical	E	$5 \times 10^{10} Pa$	Young Modulus
	G	$2.3 \times 10^{10} Pa$	Shear Modulus
Geometric	$\bar{\kappa}_1, \bar{\kappa}_2$	$1/236, 1/294$ [1/mm]	pre-curvatures of outer and inner tubes
	l_1, l_2	$200, 200$ [mm]	tube length
	$d_1(d_2), t_1(t_2)$	$1.6(1.2), 0.2(0.2)$ [mm]	outer (inner) tube's diameter and thickness

The simulation result on torsional deformation was obtained, as shown in Fig. 4a. The input angle refers to the relative twist angle $\alpha(s)$ at $s = 0$. If one tube is fixed and the other is connected a motor, the input angle is equal to the motor's rotation. The measurement of torsional deformation reported in [11] is shown too in Fig. 4a for comparison. It is seen that the two results are very close to each other.

The simulation results on the tube assembly's shape were also obtained. One result is displayed in Fig. 4b, where the pose of the tube-tip is shown together with a frame at the tip to indicate the orientation. While the simulation was carried out for single session of two-tube assembly, it could be extended to complicated configurations where more sessions of tube assemblies connected serially to build a curve of desired shape.

5 Conclusions

In this work, the shape modeling of a type of concentric-tube continuum robot was developed for an assembly of super-elastic NiTiNol tubes. A new model was developed, in which both bending deformation and torsion are considered. The model

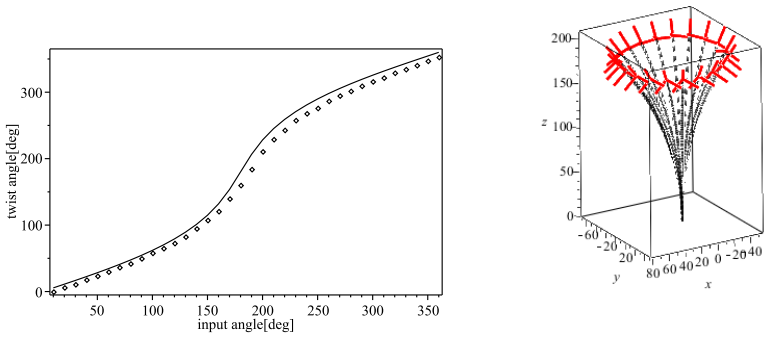

(a) (b)

Fig. 4 Simulation results: (a) twist angle simulations (solid line) compared with measurements (dots), (b) tube centerline changing with outer tube rotation. Red lines show the tube orientation

allows the calculation of the shape a tube assembly as a function of the parameters of tubes and their relative angle. The model, developed for tubes of variable curvatures, can be used in the continuum kinematic design and analysis.

References

1. M. Blessing and I.D. Walker. Novel continuum robots with variable-length sections. In *Proc. 3rd IFAC Symposium on Mechatronic Systems, Sydney, Australia*, 2004.
2. B. Mazzolai, L. Margheri, M. Cianchetti, P. Dario, and C. Laschi. Soft-robotic arm inspired by the octopus: II. from artificial requirements to innovative technological solutions. *Bioinspiration & Biomimetics*, 7(2):025005, 2012.
3. C. Li. *Design of Continuous Backbone, Cable-driven Robots*. Clemson University, 2000.
4. P. E. Dupont, J. Lock, and E. Butler. Torsional kinematic model for concentric tube robots. In *Proc. 2009 IEEE Inter. Conf. on Robotics and Automation*, pages 2964–2971, 2009.
5. R. J. Webster, III and B. A. Jones. Design and kinematic modeling of constant curvature continuum robots: A review. *Int. J. Robotics Research*, 29(13):1661–1683, 2010.
6. B. A. Jones, R. L. Gray, and K. Turlapati. Three dimensional statics for continuum robotics. In *Proc. 2009 IEEE/RSJ Int. Conf. on Intelligent Robots and Systems*, pages 2659–2664, 2009.
7. D. B. Camarillo, C. F. Milne, C. R. Carlson, M. R. Zinn, and J. K. Salisbury. Mechanics modeling of tendon-driven continuum manipulators. *IEEE Trans. Robotics*, 24(6):1262–1273, 2008.
8. H. Lang, J. Linn, and M. Arnold. Multibody dynamics simulation of geometrically exact Cosserat rods. *Multibody Dynamics*, 25:285–312, 2011.
9. P. E. Dupont, J. Lock, B. Itkowitz, and E. Butler. Design and control of concentric-tube robots. *IEEE Trans. Robotics*, 26(2):209–225, 2010.
10. M.P. do Carmo. *Differential geometry of curves and surfaces*. Prentice-Hall, 1976.
11. S. Bai and C. Chuhao Xing. Shape modeling of a concentric-tube continuum robot. In *Proc. 2012 IEEE Inter Conf on Robotics and Biomimetics (ROBIO 2012), Dec, 11-14, 2012, Guangzhou, China*, pages 116–121, 2012.